Proceedings of the
International Conference on Mechanical Engineering 2011
(ICME2011) 18-20 December 2011, Dhaka, Bangladesh

ICME11-FL-052

NUMERICAL INVESTIGATION ON THE BEHAVIOR OF MOVING LIQUID SHEET

Mohammad Ali[1], **Akira Umemura**[2] **and M. Quamrul Islam**[1]

[1] Department of Mechanical Engineering, BUET, Dhaka, Bangladesh
[2] Department of Aerospace Engineering, Nagoya University, Japan.

ABSTRACT

A numerical study has been performed to provide the physics on the capillary instabilities on liquid surface and disintegration processes of liquid sheet. A moving liquid sheet in a moving gaseous medium is considered to analyze the dynamical behavior of the liquid sheet. The problem, composed of the Navier-Stokes systems associated with surface tension forces, is solved by the Volume of Fluid (VOF) technique with a Continuum Surface Force (CSF) manner artificially smoothing the discontinuity present at the interface. The investigation reveals that before disintegration of the liquid the capillary waves become unstable and the source of making the wave unstable is inherently developed by the system. By the investigation of moving liquid sheet, two modes of forces for liquid stretching can be found; one is shear force causing the stretching of liquid by shear velocity and the other is drag force causing the stretching of liquid by gas velocity ahead the tip of the liquid sheet. Stretching of liquid by shear force causes the protrusion of liquid from the tip of liquid sheet. The surface tension force causes the tip of the sheet to become round and the aerodynamic force at the tip of the sheet controls the formation of droplet and occurrence of sheet breakup.

Keywords: VOF Method, Continuum Surface Force (CSF) Model, Liquid Sheet.

1. INTRODUCTION

Liquid fuel atomization is one of the key for technological challenges in efficient mixing of fuel with oxidizer in both low and high speed transports. Efficiency of combustion systems and attendant reduction of pollutants are dependent strongly on the degree to which fuel and oxidizer are mixed before they react. No doubt, the mixing of liquid fuel depends strongly on the subsequent fuel atomization technique and the characterization of the relevant processes for its distribution in the oxidizer. Since the process of atomization is very quick and fine, a numerical simulation is performed to understand the relevant physics as well as the mechanism of atomization. Moreover the problem is of considerable fundamental interest in the fluid mechanics for a time dependent free-boundary problem and in flow-induced deformation of a variety of flexible bodies. Several methods were proposed and in use for the simulation of such flow problems. These methods are discussed in several published literatures. Gueyffier et al. [1] described a numerical scheme for interface calculations. The authors used the volume of fluid interface tracking method and a piecewise linear interface calculation in the scheme. The method of interface tracking with the connection of volume fraction and interface position was described in detail. A model called continuum surface force (CSF) for surface tension effects on fluid motion was developed by Brackbill et al. [2]. The model interpreted the surface tension as a continuous, three-dimensional effect across an interface, rather than as a boundary value condition on the interface. Hirt et al. [3] made a short review of different methods used for embedding free boundaries and compared the relative advantages and disadvantages of these methods. The author introduced a new technique in the volume of fluid (VOF) method which worked well for complicated problems. Welch et al. [4] used a VOF based interface tracking method in conjunction with a mass transfer model and used in simulation of horizontal film boiling problem.

The formation of droplet and breakup behavior of a circular jet has been extensively investigated over the past century. An earlier account of the work is summarized by Rayleigh [5] who performed a delightful discussion on jet instability and published both theoretical and experimental results on capillary instability phenomena. In an experiment, Goedde and Yuen [6] examined the capillary instability of vertical

liquid jets of different viscosities and measured the growth rates of waves for disturbances of various wavelengths. In another investigation Donnelly and Glaberson [7] performed some experiments and discussed the effects of viscosity on the capillary instability and growth rate. Also several other investigations [8, 9] can be found in the literature which described general features on end pinching of elongated liquid drops, their deformation and breakup. Recently, Ali [10] performed an investigation on the dynamics of liquid sheet using VOF method with CSF model. All the above researchers used VOF method for two-phase flow problems with the conjunction of some other models and techniques. Therefore, it can be concluded that the VOF method is one of the popular schemes for tracking interfaces and hence implemented in present algorithm to reveal the physics of dynamics and disintegration processes of liquid column and sheet.

2. MATHEMATICAL MODELING

The flow field is governed by time dependent three-dimensional Navier-Stokes equations with surface tension force. Body forces are neglected. These equations can be expressed as

$$\frac{\partial \vec{U}}{\partial t}+\frac{\partial \vec{P}}{\partial x}+\frac{\partial \vec{Q}}{\partial y}+\frac{\partial \vec{R}}{\partial z}=\frac{\partial \vec{P}_v}{\partial x}+\frac{\partial \vec{Q}_v}{\partial y}+\frac{\partial \vec{R}_v}{\partial z}+\vec{F}_{sv} \qquad (1)$$

$$U=\begin{pmatrix}\rho\\ \rho u\\ \rho v\\ \rho w\end{pmatrix},\ P=\begin{pmatrix}\rho u\\ \rho u^2+p\\ \rho uv\\ \rho uw\end{pmatrix},\ Q=\begin{pmatrix}\rho v\\ \rho uv\\ \rho v^2+p\\ \rho vw\end{pmatrix},\ R=\begin{pmatrix}\rho w\\ \rho uw\\ \rho vw\\ \rho w^2+p\end{pmatrix}$$

$$P_v=\begin{pmatrix}0\\ \tau_{xx}\\ \tau_{xy}\\ \tau_{zx}\end{pmatrix},\ Q_v=\begin{pmatrix}0\\ \tau_{xy}\\ \tau_{yy}\\ \tau_{yz}\end{pmatrix},\ R_v=\begin{pmatrix}0\\ \tau_{zx}\\ \tau_{yz}\\ \tau_{zz}\end{pmatrix},\ F_{sv}=\begin{pmatrix}0\\ \sigma\kappa f n_x\\ \sigma\kappa f n_y\\ \sigma\kappa f n_z\end{pmatrix}$$

The following terms are expressed as,

$$\tau_{xx}=\lambda\left(\frac{\partial u}{\partial x}+\frac{\partial v}{\partial y}+\frac{\partial w}{\partial z}\right)+2\mu\left(\frac{\partial u}{\partial x}\right),$$

$$\tau_{zz}=\lambda\left(\frac{\partial u}{\partial x}+\frac{\partial v}{\partial y}+\frac{\partial w}{\partial z}\right)+2\mu\left(\frac{\partial w}{\partial z}\right),$$

$$\tau_{yy}=\lambda\left(\frac{\partial u}{\partial x}+\frac{\partial v}{\partial y}+\frac{\partial w}{\partial z}\right)+2\mu\left(\frac{\partial v}{\partial y}\right),$$

$$\tau_{xy}=\mu\left(\frac{\partial u}{\partial y}+\frac{\partial v}{\partial x}\right),\ \tau_{yz}=\mu\left(\frac{\partial w}{\partial y}+\frac{\partial v}{\partial z}\right),$$

$$\tau_{zx}=\mu\left(\frac{\partial w}{\partial x}+\frac{\partial u}{\partial z}\right)$$

$$\lambda=-\frac{2}{3}\mu.$$

Where, u, v, w are velocities in the flow field, ρ is the density, p is the pressure, μ is the viscosity, F_{sv} is the surface tension force, σ is the surface tension, κ is the curvature of surface, n is the unit normal to the surface and f is a function for continuous change of the color variable (here density) across the thickness of fluid interface.

3. NUMERICAL SCHEME

To understand the phenomena of the capillary instability and disintegration processes of liquid sheet, a numerical algorithm has been developed to solve time dependent three-dimensional Navier-Stokes equations with surface tension force. The algorithm can capture the capillary waves radiated on the surface of liquid sheet. For the simulation, VOF method with a fixed, regular, uniform grid is used to solve the problem. Piecewise Linear Interface Calculation (PLIC) is implemented for the advection of liquid interface. The treatment of surface tension consisted of artificially smoothing the discontinuity present at the interface is a Continuum Surface Force (CSF) manner [2].

To determine the fractional volume and interface position, a parameter is searched which is related to the smallest distance between the planar surface of liquid and the origin of the cell. Therefore this parameter represents the distance along the normal and also defines the planar surface of liquid in the cell. Utilizing this parameter we can determine the area of different sides of the cell occupied by the liquid. A comprehensive description of this calculation can be found in reference, Gueyffier et al. [1], where the description is started with two-dimensions and later it is generalized to three dimensions for calculation of area as well as volume of the fluid. Both area and volume calculations are continuous, one-to-one, and have a functional relationship with volume inside the cell lying below the planar surface and the parameter which characterizes the plane. For easy calculation of area and volume of the liquid, the cells are identified as three categories: (i) cells with zero value of one component of normal to the planar surface, (ii) cells with zero values of two components of normal to the planar surface, and (iii) cells with non-zero normal components. Algorithm is constructed for these categories of cells with the implementation of all possible logics. The interface where the fluid changes from one fluid to the other discontinuously is replaced by a continuous transition. It is not appropriate to apply a pressure jump induced by surface tension at the interface. Rather, the surface tension should act everywhere within the transition region. In fact, the surface tension contributes a surface pressure which is the normal force per unit interfacial area.

In present work the surface tension force is estimated by a volume force which gives the correct surface tension. The volume force is then calculated with the area integral over the portion of the interface lying within the small volume of integration. A suitable color function (density for present investigation) is chosen for smooth variation over the thickness across the interface. A detail

description and the formulation for numerical simulation can be found in reference, Gueyffier et al. [1]. The model is implemented in the algorithm for present investigation.

4. PROBLEM STATEMENTS

The schematic of the moving liquid sheet with initial setting and calculation domain is shown in Fig. 1. As liquid, sulfur hexafluoride (SF_6) of critical temperature, 318.7 K and critical pressure, 3.76 MPa is considered for moving sheet. The moving, quiescent, viscous gas medium is nitrogen with pressure of 7.0 MPa. The thickness of the liquid sheet is 0.8mm. Initial length of the liquid sheet, considered from tip of the sheet to the base, is four times of the half of the unperturbed sheet thickness "a". To remove the computational error, the tip of the liquid sheet is initially considered as round. In present study, both liquid and gas are entering into the flow field from left boundary of the calculation domain. The inlet velocity of liquid as well as the initial velocity in the liquid region is determined from liquid Weber number (We_l). The velocity distribution of liquid sheet at the inlet is rectangular as shown in Fig.1 and uniform velocity distribution is set for unperturbed liquid region. The gas velocity for the inlet boundary as well as for the initial gas region is determined from gas Weber number (We_g). At interface of liquid and gas in inlet, parabolic velocity distribution for gas is considered as shown in Fig.1 and uniform velocity distribution is set for initial gas region. For parabolic velocity distribution of gas, the boundary layer thickness is calculated by using the distance 10 times longer of the liquid sheet thickness.

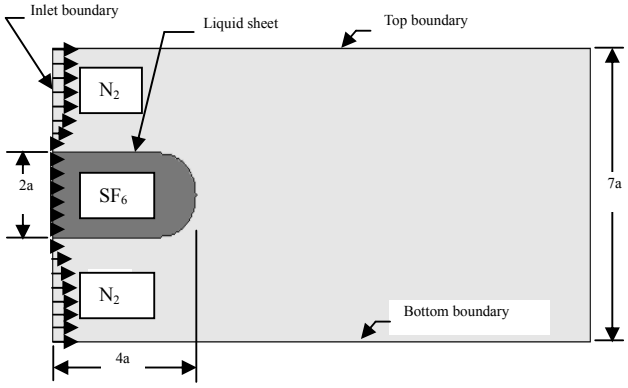

Fig 1. Schematic of unperturbed liquid sheet; a = half of liquid sheet thickness.

For this investigation the liquid Weber number, We_l = 1.0 is considered and for all through the calculation it is kept constant. The choice of this liquid Weber number is to keep the tip of the initial liquid sheet at the same location in the calculation domain even if the aerodynamic effect of gas modifies the behavior of the liquid sheet. For present calculation fixed, uniform and square grid system is considered with 300 grids along the horizontal direction and 140 grids along vertical direction. For sheet thickness 40 grid points are considered out of 140 grid points along the transverse direction. The grid size, 0.02mm is adopted for this calculation including both liquid and gas regions. Through the calculation time, the uniform gas velocity is imposed on top and bottom boundaries of the calculation domain which is same as inlet gas velocity and constant gas pressure is considered for these two boundaries as well as the inlet boundary for gas. The zero gradients of both velocity and pressure are used for outlet boundary of the calculation domain.

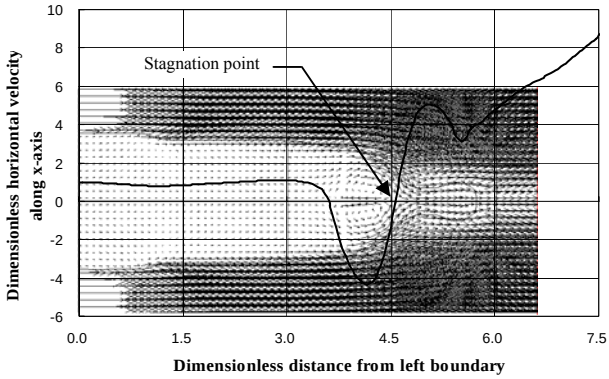

Fig 2. A part of velocity vector field and horizontal velocity along x-axis at t = 0.54 when We_g = 25

5. RESULTS AND DISCUSSIONS

Figures 2~4 show the arbitrarily magnified velocity vector field with the horizontal velocity on the mid-section of the liquid sheet at different dimensionless time. It can be pointed out that the horizontal velocity on the mid-section of the flow field is named as the horizontal velocity along x-axis for convenient presentation of the result. Figure 2 is black and white, while the others are drawn by color for easy observation. Both color and length of arrow indicate the magnitude of the velocity vector at different locations of the flow field. The red color has the highest magnitude of the velocity and the blue has the lowest. However, in different velocity vector field the length of arrow sign shows different magnitude of the velocity. The dimensionless velocity along x-axis is superimposed on each figure. It can be pointed out that the horizontal axis is made dimensionless by the ratio of actual distance to the half thickness of the unperturbed liquid sheet and the velocity is made dimensionless by the ratio of actual velocity to the square root of $\sigma/(\rho_l a)$, where ρ_l is the density of the liquid. The liquid velocity along the x-axis of the sheet as well as the gas velocity at the tip of the sheet can be understood from the curve.

Irrespective to the presence of gas flow, it is common characteristics of a liquid that the tip of liquid sheet tends to contract by surface tension. However, the large shear stress acting in gas side on both sides of the liquid sheet tends to make the liquid sheet thinner. Two effects are activated on the flow field, namely: aerodynamic effect and surface tension effect. Figure 2 shows that due to existence of shear velocity at the interface of liquid and

gas, the surface of the liquid sheet is stretched. By dint of the shear velocity, the surface liquid has higher velocity than inner liquid velocity, and changes the direction of flow at the end of the sheet. The streams of surface liquid, coming from either surface of the liquid sheet, merge with each other and form a protrusion of liquid by jet action because the resulting stagnation pressure at the tip is so high that the surface tension acting on the round tip of the initial liquid sheet can not confine the impinging liquid in the initial liquid sheet. At the same time, a pair of large recirculation (at negative central velocity region) develops inside the liquid sheet near the base of the liquid protrusion. Thus, the main function of aerodynamic effect is to make vortices and a stagnation point. An interesting feature is that, once the recirculation flow is established, the volumetric flow rate of the liquid entering the protrusion region is almost fixed. Figure 2 shows that the highest liquid velocity towards positive x-direction occurs in the liquid protrusion region. This velocity is about four times greater than the velocity of the liquid entering the calculation domain while the protrusion thickness is about one fourth of the initial liquid sheet thickness. This fact implies that the amount of liquid entering the calculation domain flows into the protrusion region. This trend continues in the subsequent time, so that the length of the liquid sheet with the same magnitude of thickness as the initial one does not change significantly throughout Figs. 2 ~ 4.

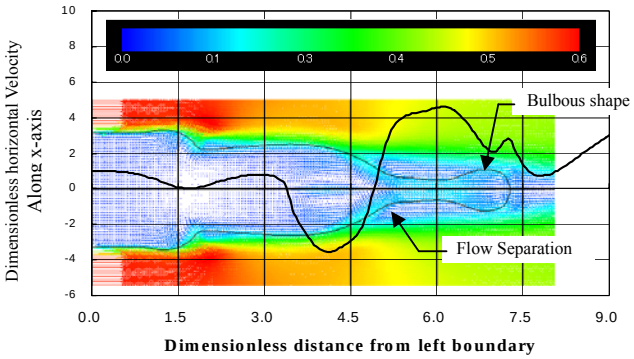

Fig 3. A part of velocity vector field and horizontal velocity along x-axis at t = 1.08 when We_g = 25

For more details on the formation of the protrusion region, the following fluid dynamic structure can be noted. The increase and decrease in liquid pressure, caused by the surface tension acting on the convex and concave surface of the liquid sheet produces centrifugal forces necessary for the liquid surface to turn the stepped shape. Therefore, the liquid entering the protrusion region continues to elongate the protrusion. On the other hand, the surface tension tends to contract the tip of protrusion and forms a surface wave due to which the tip of the protrusion attains a bulbous shape (the tip looks like as an electric bulb) shown in Fig. 3 and gradually increases the diameter of the swell. It is notable that in the protrusion region, the effect of surface tension is intensified because the thinner liquid sheet is embedded in the gaseous wake flow of the much thicker liquid sheet. The velocity in the protrusion region increases towards the tip and then decreases a little at the bulbous tip of the sheet due to a pair of recirculation formed by gas velocity. The horizontal velocity distribution also shows that the gas velocity increases continuously with the distance from the tip of the protrusion region along the horizontal direction. The reason can be explained in the way that at initial stage of the flow, the protrusion length is small and the two gas streams coming from opposite sides of the liquid sheet are merging to a common stream at the liquid sheet tip and increase the velocity. The suction of gas flow at the tip of liquid sheet helps stretching the liquid protrusion as shown in Fig. 4.

Figure 5 shows more deformation of the liquid sheet than that of Figs. 2, 3 and 4, and the remarkable change of velocity can be observed at the end of first step at location of dimensionless distances from 1.2 ~ 2.5 and at liquid protrusion region. The figure contains three steps deformation on liquid sheet surface. The first step is close to the liquid sheet entrance, the second step is at the end unperturbed liquid sheet (at dimensionless distance of 4.5), and the third step is the protrusion of liquid which contains a bulbous shape of liquid at the tip caused by surface tension. This step structure looks like stairs as shown in Fig.6. At the beginning of calculation, a pair of recirculation is produced near the tip of the sheet and makes one step. Due to initial condition of the flow field associated with the inflow conditions of both liquid and gas another step is formed at downstream of the liquid entrance as can be observed in Fig. 5. The formation of step causes the flow separation of gas near the outer edge of each step. Thus, most of the protrusion region is embedded in the separated flow region and experiences the shearing stress directing in the upstream direction.

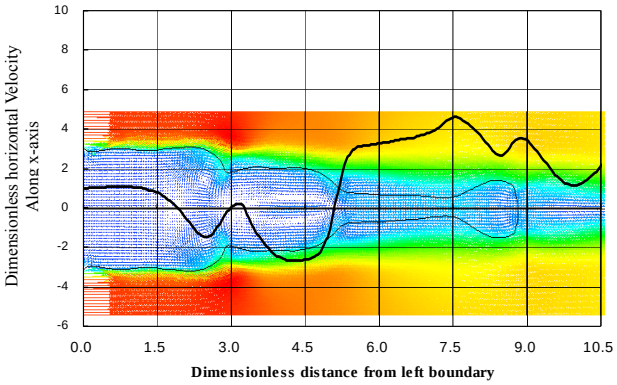

Fig 4. A part of velocity vector field and horizontal velocity along x-axis at t = 1.73 when We_g = 25

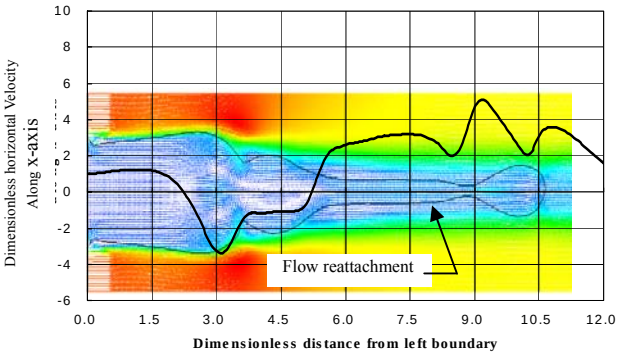

Fig 5.A part of velocity vector field and horizontal velocity along x-axis at t = 2.37 when We_g = 25

A weak propagation of capillary wave and contraction of liquid sheet caused by surface tension can be observed in Fig. 5. The development of a neck adjacent to the bulbous tip, at which the first breakup of the liquid sheet will take place at a later time of t=2.61, is apparent at this stage. The highest liquid velocity towards positive x-direction occurs at the neck, which is the consequence of mass conservation. The first step moves downstream as the new liquid enters the calculation domain. The central velocity distribution in Fig. 4 shows increase of velocity towards negative direction in the first step and decrease of negative velocity in second step. Another observation is that the shape of the liquid sheet tip in Fig. 4 tends to become flat which can be explained as follows. The change in trend of gas flow at downstream of the protrusion tip can be found in Fig. 4, which is caused by the merging action of two gas streams coming from the opposite side of the protrusion and their separation. With the increase of liquid protrusion length as well as the diameter of the bulbous shape at the tip, the separation length from the tip of sheet increases due to vitiation of main gas streams. This flow separation from the protrusion tip can be observed in Fig. 3 in which little decrease of central gas velocity at distance of 5.5 from left boundary can be found. The flattening of the protrusion tip is caused by the gas flow impinging on the tip. Figure 5 is the velocity vector field at dimensionless time, t = 2.38 which is near to the breakup time, t = 2.61. The flow of gas separated at second step, tends to reattach with the liquid surface at the later half of the protrusion part. Due to surface tension effect and the dynamical behavior of gas to form step, the upstream portion of the neck tends to form a pair of weak recirculation and a stagnation point which cause high pressure and low velocity in the upstream region of neck as shown in Fig. 5. Due to the recirculation and flow stagnation, the neck is destabilized and breaks up.

The close observations of the flow field near the breakup time t=2.51 are required to describe and understand the breakup processes. Accordingly, Fig. 7 shows the distributions of dimensionless velocity and pressure along x-axis for time, t=2.51. In Fig. 7 the dimensionless velocity and pressure on the mid-section are termed as non-dimensional axial velocity and

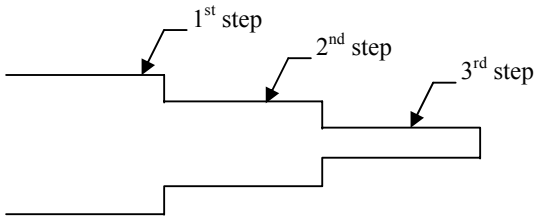

Fig 6. The structure of steps tends to develop by aerodynamic effect.

pressure, respectively. The liquid pressure shown in the figure is obtained by subtracting the gas pressure of the calculation domain and expresses the pressure developed only by the aerodynamic force and surface tension. The remarkable changes occur around the neck of the tip wave. It can be observed that immediately upstream of the neck, the central horizontal velocity decreases rapidly with time while the pressure increases. The stagnation point can be understood by observing the pressure distribution curve. It can be pointed out that the gas, which separates from the second step, reattaches upstream of the neck when the length of the protrusion region increases beyond a certain length. After this reattachment, the gas flow tends to create another step at the neck of the capillary wave which causes a pair of weak recirculation and a stagnation point upstream of the neck. Due to recirculation and stagnation point in the thin liquid sheet, very low velocity of liquid can be observed in the distribution of velocity. The jet action for aerodynamic effect of gas causes high velocity of liquid immediately after the neck. With time marching, the recirculation at upstream of the neck intensifies and causes reverse flow of liquid. Moreover, the stagnation point increases the pressure which constricts the liquid flow towards positive x-direction. Thus, the formation of step, pair of vortices, and stagnation point in the thin portion of liquid sheet cause the breakup of the liquid sheet.

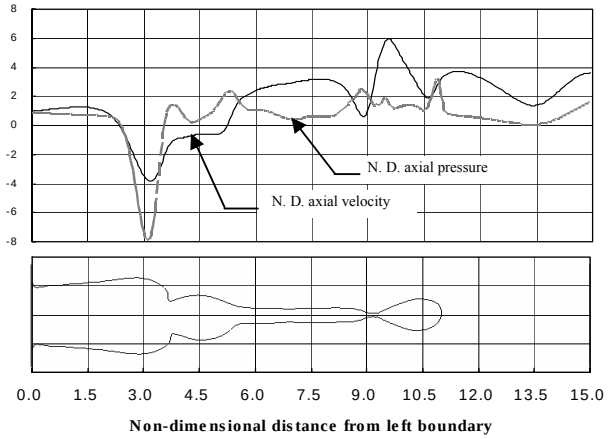

Fig 7. Non-dimensional horizontal velocity and pressure distributions along x-axis at time, t=2.51, We_g = 25.

6. CONCLUSIONS

A numerical analysis has been performed to investigate the mechanism of sheet breakup and the dynamics involved in the breakup processes. From this investigation it can easily be understood that the co-flowing gas stretches the liquid sheet and produces the protrusion of the liquid from the tip of the sheet by jet action of the stretching liquid. Due to stretching and protrusion of liquid, steps like stairs are formed on the sheet surface. The gas then acts on the steps and forms a pair of vortices and stagnation point near the end of each step. It can be found that the vortices and stagnation point play the main role for the breakup of the liquid sheet.

The results show that the capillary wave takes the initiation to form the step by gas flow for breakup. It can be observed that the thickness of liquid protrusion is small and surface tension generates the capillary wave on the tip of the protrusion. Naturally, a capillary wave contains swell and neck. This neck helps the flow of gas form a step on the neck. Finally the step is followed by a pair of weak vortices and stagnation pressure which resist the flow of liquid through the thin sheet and eventually the breakup occurs.

ACKNOWLEDGEMENTS

The authors gratefully acknowledge the computing facilities in the department of Mechanical Engineering, Bangladesh University of Engineering and Technology (BUET) to conduct this research work.

7. REFERENCES

1. Gueyffier, D., Li, J., Nadim, A., Scardovelli, R. and Zaleski, S., "Volume-of-Fluid Interface Tracking withSmoothed Surface Stress Methods for Three-Dimensional Flows", J. Computational Physics, 152, pp. 423-456, 1999.
2. Brackbill, J. U. Kothe, D. B. and Zemach, C., "A Continuum Method for Modeling Surface Tension", J. Computational Physics, 100, pp. 335-354, 1991.
3. Hirt, C. W. and Nichols, B. D., "Volume of Fluid (VOF) Method for the Dynamics of Free Boundaries", J. Computational Physics, 39, pp. 201-225, 1981.
4. Welch, S. W. J. and Wilson, J., "A Volume of Fluid Based Method for Fluid Flows with Phase Change", J. Computational Physics, 160, pp. 662-682, 2000.
5. Rayleigh, L., "On the Capillary Phenomena of Jets". Proceedings of the Royal Society of London, 29, 1879, pp. 71-97.
6. Goedde, E. F. and Yuen, M. C., "Experiments on Liquid Jet Instability", J. Fluid Mech., 40, part 3, 1970, pp. 495-511.
7. Donnelly, R. J. and Glaberson, W., "Experiments on the Capillary instability of a liquid Jet", Proceedings of the Royal Society of London, Series A, 290, 1966, pp. 547-556.
8. Stone, H. A., Bently, B. J. and Leal, L. G., "An Experimental Study of Transient Effects in the Breakup of Viscous Drop", J. Fluid Mech., 173, 1986, pp. 131-158.
9. Stone, H. A. and Leal, L. G., "Relaxation and Breakup of an Initially Extended Drop in an Otherwise Quiescent Fluid", J. Fluid Mech., 198, 1989, pp. 399-427.
10. Ali, M., Dynamical Behavior of Liquid Sheet with Co-flowing Gas, Project report, CASR, Bangladesh University of Engineering and Technology, April, 2010.

8. MAILING ADDRESS

Dr. Mohammad Ali
Professor
Department of Mechanical Engineering
BUET, Dhaka-1000, BANGLADESH.
Phone : 88029665636,
88029665650-80 (Extn. 7511),
88-01732-194776 (cell).
FAX : 880-2-8613046, 880-2-8613026.
E-mail : mali@me.buet.ac.bd